# Numerical Optimization of the Ultrasonic Cleaning Technique for Pipelines

Habiba Lais[1], Jamil Kanfoud[1] and Tat-Hean Gan[1]
1. Brunel Innovation Centre, Brunel University London, Uxbridge, UB8 3PH

## Introduction

Fouling build up is a well-known problem in various industries [1]-[2]. Accumulation of fouling occurs in different structures, e.g. offshore pipes, ship hulls, floating production platforms. The type of fouling that accumulates is dependent on environmental conditions surrounding the structure itself. Current methods deployed for fouling removal span across hydraulic, chemical and manual, all sharing the common disadvantage of necessitating halting production for the cleaning process to commence. Conventionally, ultrasound is used in ultrasonic baths to clean a submerged component by the generation and implosion of cavitation bubbles on the fouled surface. However, this requires the submersion of the fouled structure and thus may require a halt to production. Large fouled structures such as pipelines may not be accommodated. The application of high power ultrasonics is proposed in this work as a means to remove fouling on a structure whilst in operation.

## Ultrasonic Cleaning Technique

The technique itself is carried out by using High Power Ultrasonic Transducers (HPUT) with a bespoke contact surface, which are attached to the outer wall of a structure (submerged/filled with liquid). The excitation of the HPUT at its known natural resonant frequency generates cavitation bubbles within the liquid where the implosion of these bubbles may occur on the surface of the fouling and result in fouling removal

## FEA Theory and Methodology

To assist with understanding how wave propagation can promote larger coverage of fouling removal over a structure, an FEA model was created in COMSOL Multiphysics 4. The model consists of a Langevin transducer placed on a stainless steel pipe, matching the dimensions and material properties of the experimental specimen.

Several COMSOL physics modules are incorporated into the model to account for the transducer excitation through the solid pipe wall and into the fluid domain. The specific physics used are as follows:

- Pressure Acoustics, Transient
- Electrostatics
- Solid Mechanics
- Piezoelectric Effect
- Acoustic-Structure Boundary

For the Pressure Acoustics, this is assigned to the fluid domain and uses the wave equation:

$$\frac{1}{\rho c^2}\frac{\partial^2 p_t}{\partial t^2} + \nabla \cdot \left(-\frac{1}{\rho}(\nabla p_t - q_d)\right) = Q_m \qquad (1)$$

where, $\rho$ is the total density, $p_t$ is the total pressure, $\rho c^2$ is the bulk modulus, $q_d$ is the dipole source and $Q_m$ is the monopole source.

The monopole source can be found using the following equation:

$$|p(r)| = i\rho c\frac{Qk}{4\pi r} \qquad (2)$$

where, p is the pressure amplitude, r is the distance, $\rho$ is the density of water, c is the speed of sound, Q is the source strength, k is the wave number.

The dipole source is found using the following equation:

$$|p(r)| = \left|-i\rho c\frac{Qk^2 d}{4\pi r}\cos\theta\right| \qquad (5)$$

where, d is the horizontal distance between two sources and θ is the angle between them.

The sound pressure level settings use the reference pressure for the selected fluid. The model is also set to atmospheric pressure and temperature. The transient pressure acoustic model is set to be *linear elastic* and exhibits the speed of sound and density from the material assigned to the fluid domain. The fluid has linear elastic behavior governed by

Newton's second law while solid mechanics physics is applied to the rest of the model as these components are solid. The physics is governed by the Navier equation:

$$\rho \frac{\partial^2 u}{\partial t^2} = \nabla \cdot FS + F_V \quad (3)$$

where, $\rho$ is the fluid density, $u$ is the velocity of the fluid, $F$ is the deformation gradient, $F_v$ is a body force, $S$ is the second Piola-Kirchhoff stress tensor.

All solid parts excluding the piezoelectric ceramic rings will obey their material properties and are considered to be of linear elastic material. Piezoelectric material is assigned to the piezoelectric ceramic rings which obey the solid mechanics governing equations and, additionally, the PZT-linearized constitutive equations in stress-charge form:

$$T = c_E \cdot S - e^t \cdot E \quad (4)$$

$$D = e \cdot S + \varepsilon_S \cdot E \quad (5)$$

where, $T$ is the tensor stress field, $S$ is the strain field, $E$ is the electrical field component, $D$ is the electric displacement field, $c_E$ is the elasticity matrix, $e$ is the piezoelectric coupling coefficient for the stress-charge form, $\varepsilon_S$ is the permittivity matrix. The subscripts $E$ and $S$ denote constant electric field and strain, respectively.

Electrostatic phenomena are included only in the piezoelectric ceramic rings where the signal is applied using the following formula:

$$\nabla \cdot D = \rho_V \quad (6)$$

$$E = -\nabla V \quad (7)$$

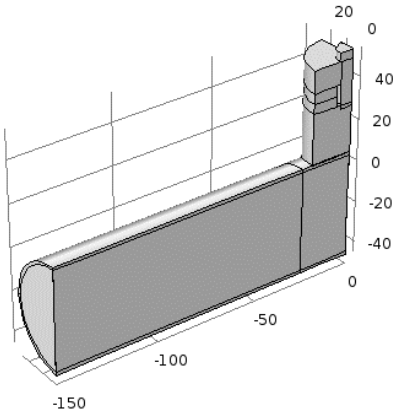


**Figure 1:** geometry of COMSOL model displaying cut planes at lines of symmetry for computation efficiency

where, $\nabla \cdot D$ is the electric charge density, $\rho_V$ is the electric charge concentration and $E$ is the electric field due to the electric potential $V$.

The terminal and ground equipotential are applied to the boundaries explicitly as previously specified. The ground boundary is set equal to 0 V and the terminal boundary is set to:

$$V = V_0 \quad (8)$$

where, $Vo$ is the modulating 40 kHz, 500Vpk-pk sine waveform to replicate the signal generated in the experimental setup as explained in Section III. Correct polarization is achieved by assigning a rotated global co-ordinate system to change the direction of polarization of one of the piezoelectric ceramic rings.

Multiphysics modules are assigned to couple the pressure acoustics and solid mechanics physics across the acoustic-structure boundary between the fluid and solid domain. This allows the radiation of the wall due to transducer excitation to be taken into account and create high and low pressure to propagate into the fluid domain [3]. For this reason, COMSOL is used to incorporate required physics to simulate the experimental configuration for the present study.

In the experiment, the coupling of the transducer contact surface to the pipe surface is done by applying acoustic couplant gel between the contact surface of the transducer and pipe to remove any air bubbles which can affect the ultrasonication performance. The COMSOL model mimics this attachment by using integration on the boundary between the transducers contact surface and pipe surface. A fixed constraint is placed on the top of the transducer and the transducer holder is ignored within the model.

A dynamic transient simulation to map out the propagation of the wave requires the calculated mesh to be optimal. The wave equation requires the time stepping within the solver to complement the meshing itself to yield an accurate solution. The meshing size requires five 2nd-order mesh elements per wavelength. The equation used to calculate the maximum allowed mesh element size (*ho*) [4] is given by:

$$h_o = \frac{c}{N f_o} \quad (9)$$

where, $c$ is the velocity, $N$ is number of elements per wavelength and $f_0$ is the center frequency.

*Free Tetrahedral* elements are used for a high density around the transducer location, the remainder of the geometry is swept as follow (10),

$$Sweep\ density = \frac{2800mm}{h_o} \quad (10)$$

The selected study for this model is *Transient*, so that the simulation can generate results as the modulated sine wave propagates from the transducer.

The increments are based on the maximum allowed mesh element size. The time steps are chosen to resolve the wave equally over time whilst the meshing is placed to resolve the wave propagation over the model itself. Time steps must be optimized relative to the mesh and this is supported with the relationship between mesh size $h_0$ and time step (Δt):

$$t_x = \frac{c\Delta t}{h_o} \quad (11)$$

The $t_x$ ratio is given as 0.2 as it is suggested to be near optimal and by rearranging the equation (11), the time steps are calculated using (12):

$$\Delta t = \frac{t_x h_o}{c} = \frac{0.2 h_o}{c} \quad (12)$$

The modelled pipe specimen is a Stainless Steel 315L pipe which is 300 mm in length, 1.5 mm in wall thickness and 50.08 mm in outer diameter. The model assumes two lines of symmetry as shown in Figure 1. A single quadrant of the pipe is modelled to reduce the computation size.

## FEA Results and Validation

The fouling removal experiment examines a stainless steel pipe with a thin layer of calcite on the inner wall. The excitation from a HPUT was used to clean an area of the calcite from the inner pipe wall whilst measuring outer wall displacements using the 3D-LDV. Vibrometry analysis shows high displacement at the locations of fouling removal of the pipe sample.

To validate the model, the predicted pipe displacement is compared with the Vibrometry results. Figure 1 shows the comparison of the cleaned area with Vibrometry scan and COMSOL model. Each set of results show an overlap of high displacement where cleaning results were achieved. The developed model shows a good agreement between high displacements and cleaning patterns. The model results in Figure 1 shows high displacements propagating from the transducer and localized at the circumference of the pipe perpendicular to the transducer attachment. The direction of propagation is due to the transducer producing compressional waves.

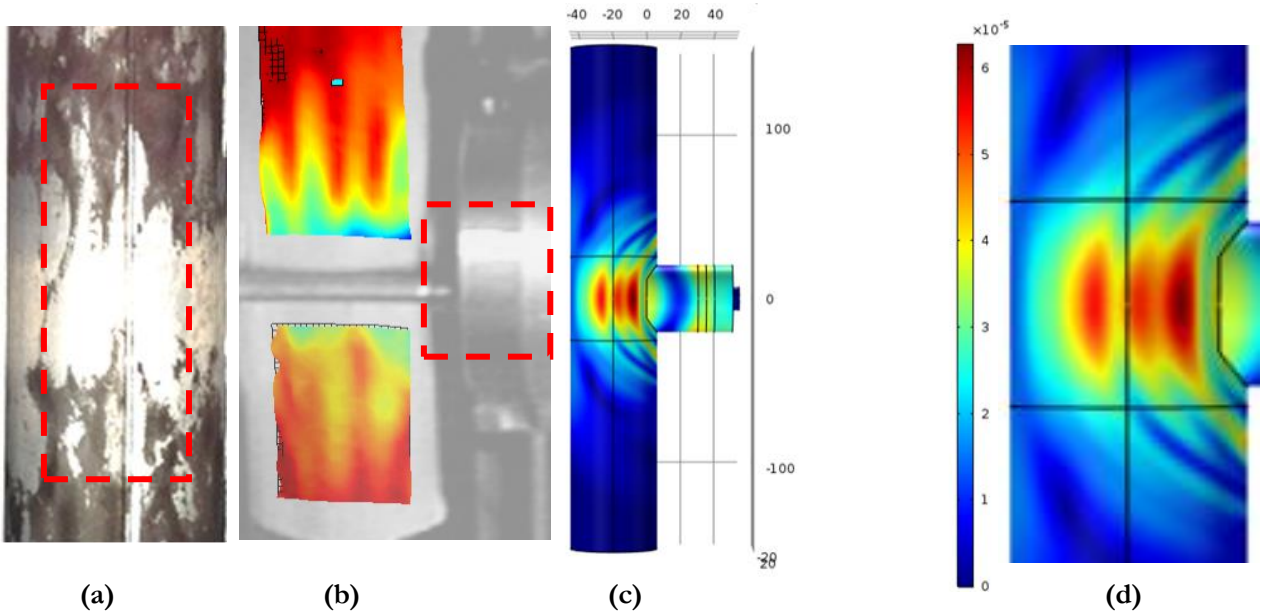


**Figure 2**: comparison of results (a) experimentally obtained localized cleaning after one cycle of ultrasonic cleaning, (b) 3D displacement measured during ultrasonic cleaning using 3D-LDV, (c) numerical simulation results and (d) zoomed version of (c) displaying high displacement achieved at same location of cleaning and 3D-LDV results

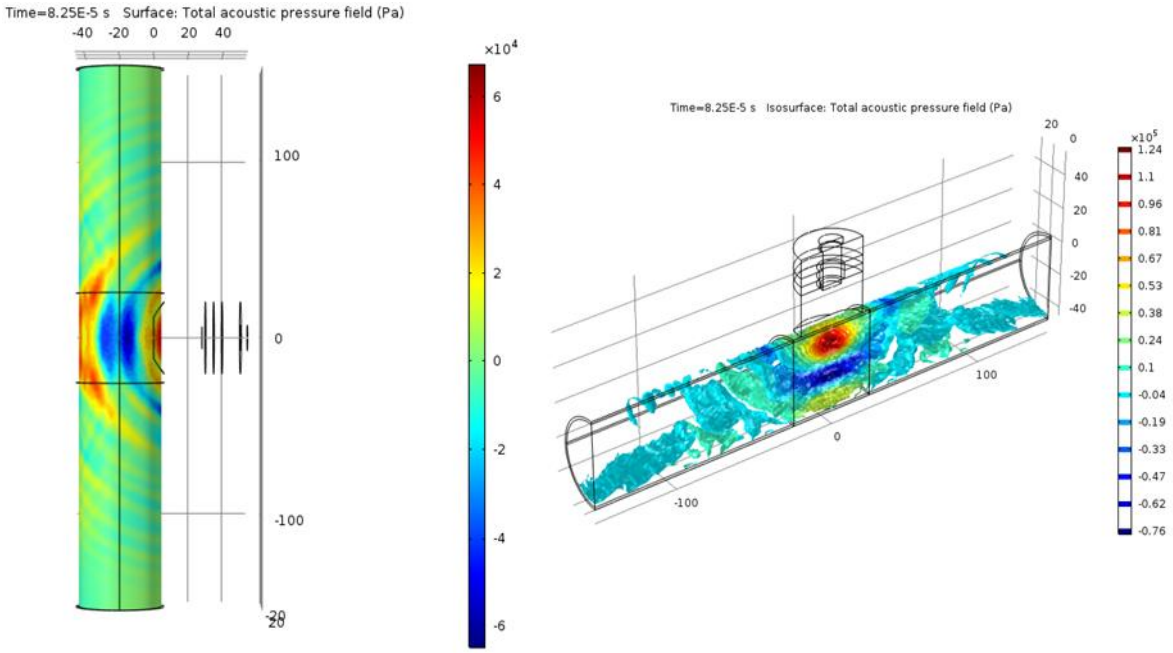


**Figure 3**: numerical results displaying surface acoustic pressure and isosurface of pipe filled with water at 825 ms

As the model validates the cleaning patterns, the next step is to validate whether an arbitrary experimental set-up is generating cavitation bubbles prior to undergoing experiments using the pressure threshold. Since this set-up has shown to achieve cavitation generation for the cleaning results to be obtained, the COMSOL model is assumed to be generating cavitation.

The total acoustic pressure is shown in Figure 3 for the same time instant as in Figure 2, as stated previously, a minimum of 1-2 Bar must be applied by the transducer to create acoustic cavitation [5]. The results show the surface of the transducer to have achieved a pressure value above 5 Bar, thus meeting the requirement for producing acoustic cavitation. The pressure then propagates in the liquid and spans the location of cleaning.

As the pressure continues propagating throughout the liquid, instants of high positive and negative pressure are in-lined with the cleaning pattern. The negative pressure instants can be linked to the rarefactions within the liquid where cavitation bubbles are generated and the positive pressure instants relate to the compressional locations in which the generated bubbles implode.

## Numerical Parametric Study

The validated numerical methodology is applied to a 6 meter long, Schedule 40, 6 inch diameter, carbon steel pipe. This thesis conducts a parametric study to investigate the optimal HPUT array (see Figure 4) with water filled within the pipe (static). The model focuses on a 40 kHz Langevin bolt-clamped HPUT due to its successful cleaning in prior experiments [6]–[8]. The pipe is monitored at different locations along its length. The points are placed at 1 m distances on the inner and outer walls of the pipe to monitor the acoustic pressure within the liquid and the solid displacement on the outer wall of the pipe.

The numbers of transducers being investigated are 1 (90°), 2 (90° and 270°) and 4 (0°, 90°, 180° and 270°).

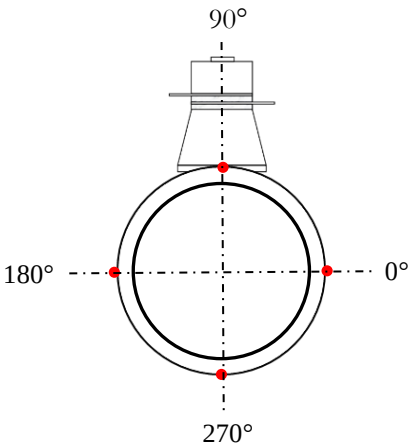


**Figure 4:** illustration of HPUT configurations for FEA analysis

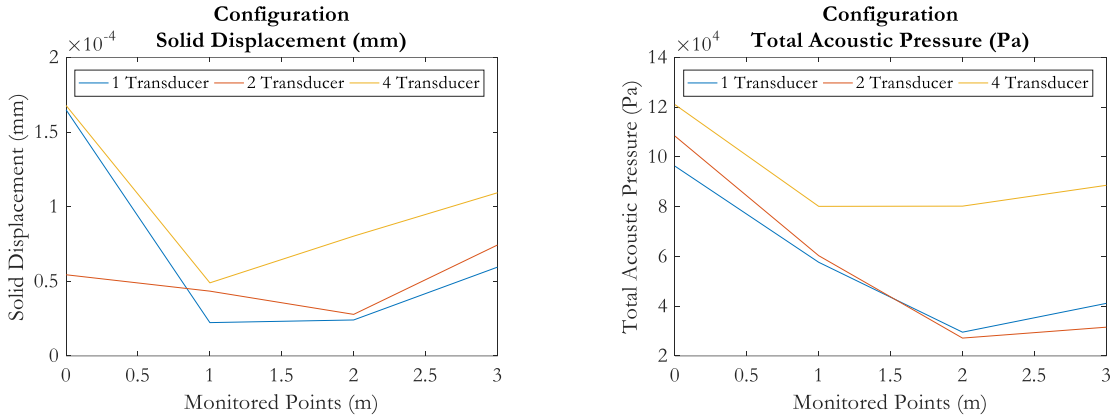


**Figure 5:** Maximum solid displacement and total pressure acoustic at monitored points for each investigated transducer configuration

## Optimisation Results and Analysis

The results of the FEA parametric study were compiled to compare the solid displacement and total acoustic pressure at monitored points along the length of the pipe (0, 1, 2, 3 m).

To compare the coverage and amplitude achieved from each configuration, the maximum amplitude of solid displacement and total acoustic pressure is measured from the monitored points along the length of the pipe. Polar plots are created for each configuration at the maximum amplitude at different locations to analyse the coverage over the cross-section of the pipe wall.

Comparing the amplitude at the monitored points for the different configurations in Figure 5, the trend shows that the 1-HPUT achieves its maximum displacement and acoustic pressure amplitude at the transducer location; along the length of the pipe, the 1-HPUT case reduces in amplitude, resulting in an average acoustic pressure of 3 KPa.

Comparing each configuration at the excitation location, the 2-HPUT case achieved the lowest displacement, due to the configuration resulting in superposition of the signals. The remainder of the 2-HPUT results follows a similar trend to the displacement amplitude achieved for the 1-HPUT case.

For the total acoustic pressure, with the increase of HPUT, the achieved amplitude at the transducer location also increases. For the remainder of the pipe length, the 1- HPUT and 2- HPUT case follow a similar trend with an average of 3 KPa.

The 4- HPUT case has shown to achieve the highest displacement and total acoustic pressure at each monitored point, averaging 8 KPa for the remainder of the pipe length.

The polar plots in Figure 6 for the 1- HPUT case show high amplitude at the transducer location for both the displacement and total acoustic pressure. For the remainder of the circumference, the displacement averages below 0.5 x $10^{-4}$ mm. the acoustic pressure shows some peaks reaching 4 KPa at 0° and 180°. The remainder of the circumference has an average of 2 KPa of pressure being achieved. This coverage is not ideal for long distance due to the drop in amplitude and the lack of uniform coverage being achieved.

The 2- HPUT case achieves its highest amplitude at the HPUT locations (90° and 270°) as shown in Figure 7. Over the length of the pipe, the amplitude of these peaks drop. The remainder of the circumference averages below 0.5 x $10^{-4}$ mm and 5 KPa. At 0° and 180°, the peak achieved in the total acoustic pressure shows a blunt feature, which could be due to superposition related to the HPUT spacing.

The highest amplitude for the displacement and total acoustical pressure is achieved in the 4- HPUT configuration at 0°, 90°, 180° and 270° as shown in Figure 8. The configuration achieved a more uniform coverage as well as higher averaging coverage for the displacement (1 x $10^{-4}$ mm), doubling the average shown in the 1- HPUT and 2- HPUT cases. The acoustic pressure averages approximately 7 KPa.

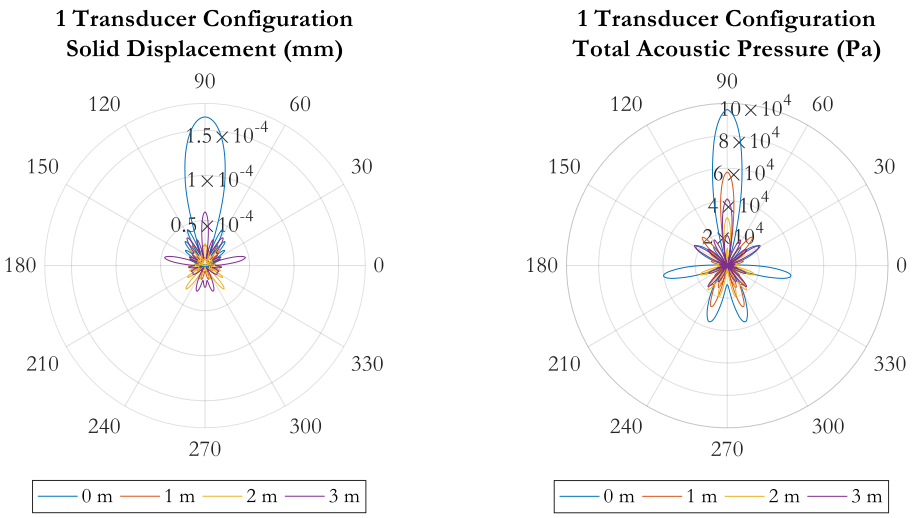


**Figure 6:** Solid displacement and total acoustic pressure polar plots for 1 HPUT case, displaying the maximum amplitude at each monitored point

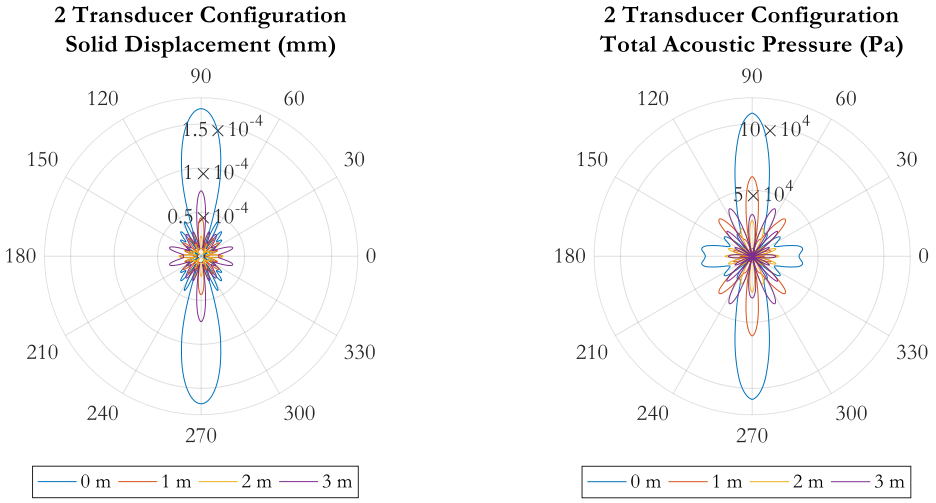


**Figure 7:** Solid displacement and total acoustic pressure polar plots for 2 HPUT case, displaying the maximum amplitude at each monitored point

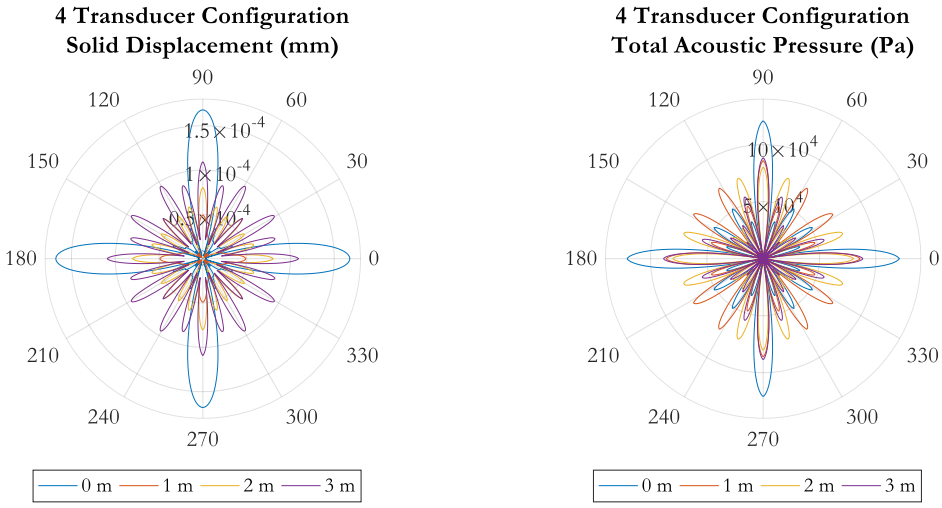


**Figure 8:** Solid displacement and total acoustic pressure polar plots for 4 HPUT case, displaying the maximum amplitude at each monitored point

## Conclusions

This work has developed an FEA model which can be used to predict and optimise cleaning patterns achieved in a pipeline. The validated model is has shown that the number of HPUTs within an array at the transducer location should typically achieve the same displacement due to the vibration of the transducer but the 2- HPUT case has a reduction as mentioned previously due to superposition. The increase in the number of HPUT improves the coverage achieved at the HPUT location and has increased the acoustic pressure within the fluid domain. The 4- HPUT case has also shown to achieve high amplitudes at further distances compared to the 1-HPUT and 2- HPUT cases showing its promise for achieving long distance cleaning coverage.

## Acknowledgements

The authors would like to give their thanks to Adrian Waka of Brunel University London for his contributions to this work.

## References

[1] A. S. Paipetis, T. E. Matikas, D. G. Aggelis, and D. Van Hemelrijck, *Emerging technologies in non-destructive testing V*. CRC Press [Imprint], 2012.

[2] L. Yang, H. Fu, H. Liang, Y. Wang, G. Han, and K. Ling, "Detection of pipeline blockage using lab experiment and computational fluid dynamic simulation," *Journal of Petroleum Science and Engineering*, p. 106421, 2019.

[3] K. Yasui, T. Kozuka, T. Tuziuti, A. Towata, Y. Iida, J. King, and P. Macey, "FEM calculation of an acoustic field in a sonochemical reactor," *Ultrasonics Sonochemistry*, vol. 14, no. 5, pp. 605–614, 2007.

[4] P. S. Lowe, R. M. Sanderson, N. V. Boulgouris, A. G. Haig, and W. Balachandran, "Inspection of cylindrical structures using the first longitudinal guided wave mode in isolation for higher flaw sensitivity," *IEEE Sensors Journal*, vol. 16, no. 3, pp. 706–714, 2016.

[5] K. Yasui, "Acoustic Cavitation," in *Acoustic Cavitation and Bubble Dynamics*, Springer, 2018, pp. 1–35.

[6] H. Lais, P. Lowe, J. Kanfoud, and T.-H. Gan, "Advancements in fouling removal using high power ultrasonics for industrial applications," in *IEEE International Conference on Industrial and Information Systems (ICIIS)*, 2017, pp. 1–6.

[7] H. Lais, P. S. Lowe, T.-H. Gan, and L. C. Wrobel, "Numerical modelling of acoustic pressure fields to optimize the ultrasonic cleaning technique for cylinders," *Ultrasonics Sonochemistry*, vol. 45, pp. 7–16, 2018.

[8] H. Lais, P. S. Lowe, J. Kanfoud, and T.-H. Gan, "Application of High Power Ultrasonics for Fouling Removal in Submerged Structures," in *IEEE/MTS OCEANS 17 Conference, Aberdeen*, 2017.